Int. J. Nano Dimens. 6 (4): 351-362, Autumn 2015
ISSN: 2008-8868

Contents list available at **IJND**

International Journal of Nano Dimension

Journal homepage: *www.IJND.ir*

Study of the flexural sensitivity and resonant frequency of an inclined AFM cantilever with sidewall probe

M. Abbasi*

School of Mechanical Engineering, Shahrood Branch, Islamic Azad University, Shahrood, Iran.

Received 06 November 2014
Received in revised form
11 February 2015
Accepted 05 March 2015

* Corresponding author:
Mohammad Abbasi
School of Mechanical Engineering, Shahrood Branch, Islamic Azad University, Shahrood, Iran.
Tel +98 9151250720
Fax +98 2332394530
Email *m.abbasi28@yahoo.com*

ABSTRACT

The resonant frequency and sensitivity of an atomic force microscope (AFM) cantilever with assembled cantilever probe (ACP) have been analyzed and a closed-form expression for the sensitivity of vibration modes has been obtained. The proposed ACP comprises an inclined cantilever and extension, and a tip located at the free end of the extension, which makes the AFM capable of topography at sidewalls of microstructures. Because the extension is not exactly located at one end of the cantilever, the cantilever is modeled as two beams. In this study, the effects of the interaction stiffness and damping, and also some geometrical parameters of the cantilever on the resonant frequencies and sensitivities are investigated. Afterwards, the influence of the interaction stiffness and damping, and the geometrical parameters such as the angles of the cantilever and extension, the connection position of the extension and the ratio of the extension length to the cantilever length on the sensitivity and resonant frequency are investigated. The results show that the greatest flexural modal sensitivity occurs at a small contact stiffness of the system, when the connection position and damping are also small. The results also indicate that at low values of contact stiffness, an increase in the cantilever slope or a decrease in the angle between the cantilever and extension can rise the resonant frequency while reduces the sensitivity.

Keywords: *Atomic force microscope; Assembled cantilever probe; Inclined cantilever; Resonant frequency; Sensitivity.*

INTRODUCTION

The resonant frequency and sensitivity of an atomic force microscope (AFM) cantilever with assembled cantilever probe (ACP) have been analyzed and a closed-form expression for the sensitivity of vibration modes has been obtained. The proposed ACP comprises an inclined cantilever and extension, and a tip located at the free end of the extension, which makes the AFM capable of topography at sidewalls of microstructures. Because the extension is not exactly located at one end of the cantilever, the cantilever is modeled as two beams. In this study, the effects of the interaction stiffness and damping, and also some geometrical parameters of the cantilever on the resonant frequencies and sensitivities are investigated.

Afterwards, the influence of the interaction stiffness and damping, and the geometrical parameters such as the angles of the cantilever and extension, the connection position of the extension and the ratio of the extension length to the cantilever length on the sensitivity and resonant frequency are investigated. The results show that the greatest flexural modal sensitivity occurs at a small contact stiffness of the system, when the connection position and damping are also small. The results also indicate that at low values of contact stiffness, an increase in the cantilever slope or a decrease in the angle between the cantilever and extension can rise the resonant frequency while reduces the sensitivity.

The atomic force microscope (AFM) is not only a powerful tool for imaging surface topography, but thanks to recent technical advances, it has proven to be the most frequently used scanning probe method for the characterization, manipulation and modification of a variety of materials such as DNA, antibodies, polymers, and silicon surfaces [1-4].

When a tip scans across a sample surface, it induces a dynamic interaction force between the tip and the surface [5]. The imaging rate and contrast of topographic images are notably influenced by the resonant frequency and the sensitivity of AFMs, respectively [6]. Dynamic responses of the AFM cantilever have been investigated by many researches [7-9].

In practice, it is very hard to keep the cantilever in parallel with the sample surface, causing an angle between the cantilever and the sample surface [10]. Taking into account the angle between the cantilever and the surface, Abbasi and Karami Mohammadi [11] found that the effect of the cantilever slope in vibration behavior of an AFM cantilever is considerable.

The normal and lateral interactive forces between the cantilever tip and the sample surface can be modeled by a set combination of a spring parallel to a dashpot in the normal direction and a similar combination in the lateral direction [12]. The interactive damping of a cantilever beam at the boundary can affect the motion of the beam. Chang [12] analyzed the effect of interactive damping on the sensitivity of flexural and torsional vibration modes of an atomic force microscope (AFM) rectangular cantilever. Mahdavi *et al.* [13] analyzed the flexural vibration modes of the AFM rectangular cantilever, taking into account the effects of RI and SD of the beam and mass and rotary inertia of the tip. Considering the coupling of the lateral and torsional vibrations of an AFM cantilever, Lee and Chang [14] studied the influence of contact stiffness and also the ratio of the tip length to the cantilever length on the resonant frequency and coupled lateral bending-torsional sensitivity of AFM rectangular cantilever. Recently, the dynamic behavior of an inclined non-uniform cantilever vibrating in fluid is studied by Lin [15]. Korayem *et al.* [16] investigated the effect of capillary force on the dynamics of tapping mode AFM when it is operated in air.

Conventional AFMs consist of microcantilevers with sharp conical or pyramidal tips located at their free ends that play an important role in nanoscale surface measurement [17]. Unfortunately, their probe tips never come in close proximity to sidewalls, no matter how sharp and thin the tips are. Therefore, nanoscale surface measurements at sidewalls are urgently demanded. In order to overcome the limitations of conventional AFMs, Dai et al. [18] proposed assembled cantilever probes (ACPs) for the direct and non-destructive sidewall measurement of nano- and microstructures. Chang et al. [19] analyzed the resonant frequency and flexural sensitivity of a form of AFM ACP proposed by Dai et al. [18], which consists of a horizontal cantilever and a vertical extension located at its free end. But for convenience, they did not take into account the effects of angle, damping and contact position of extension. Abbasi and Karami Mohammadi [20] also investigated the resonant frequency and sensitivity of the flexural modes of this ACP utilizing the nonlocal beam theory. Kahrobaiyan et al. [21] investigated the resonant frequencies and flexural sensitivities of another form of ACPs proposed by Dai et al.[22]. Abbasi and Afkhami [17] analyzed the resonant frequency and sensitivity of a caliper formed with assembled cantilever probes based on the modified strain gradient theory.

In this paper, the sensitivity and resonant frequency of the flexural vibration modes of a more comprehensive model of an assembled cantilever probe proposed by Die *et al.* [18], consisting of an inclined AFM cantilever and an extension, are analyzed. Because the size of AFM cantilever and extension are so small, in practice, it is very hard to

control the exact position of the extension and the angles of the cantilever and the extension. Therefore, we assume that the extension is not vertical and is not located exactly at the free end of the cantilever and also the cantilever has a small inclination. Finally, the influence of the interaction stiffness and damping, and the geometrical parameters such as the angles of the cantilever and extension, the connection position of the extension and the ratio of the extension length to the cantilever length on the sensitivity and resonant frequency are assessed.

EXPERIMENTAL

Computational Method

The proposed kind of AFM ACP developed in the present study, comprises an inclined cantilever and an extension near the free end, and a tip located at the free end of the extension is capable of probing in a direction perpendicular to sidewall. The geometrical parameters and configuration of this ACP are depicted in Figure 1. Both the cantilever and the extension have a uniform cross section thickness b, width a, which length is L and H, respectively, and the small length tip is h. The angle between the cantilever and the sample surface is θ and between the cantilever and extension is α. L_1 and L_2 are the lengths of the cantilever on the left and right sides of the extension, respectively. x is the coordinate along the cantilever and $w(x,t)$ is the cantilever vertical displacement along the y axis, as shown in the Figure 1. Considering the ratio of the extension rigidity to cantilever rigidity, the deflection of the extension in comparison with the cantilever deflection can be neglected, so it can be assumed that the extension is rigid. The coordinate system of p and q is parallel and perpendicular to the plane, respectively. The cantilever is clamped at $x = -L_1$, while at x = 0 has an extension and is free at $x = L_2$. Moreover, the cantilever of ACP experiences flexural vibrations during contact with the sample. The ACP interacts with the sample by a normal spring K_n a normal dashpot C_n, a lateral spring K_l and a lateral dashpot C_l.

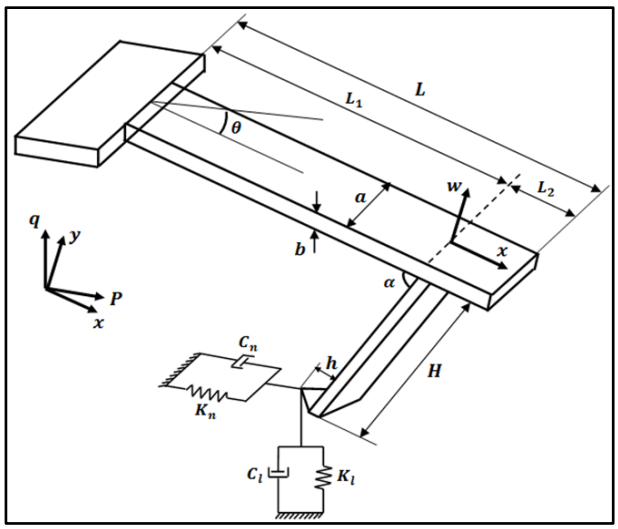

Fig. 1. Schematic diagram of an AFM cantilever microassembled with a vertical extension at the free end and a tip located at the free end of the vertical extension.

In this work, the inclined cantilever and extension are considered as an elastic beam. The inclined cantilever of ACP will vibrate flexurally. The linear differential equation of motion for the free vibration of the horizontal cantilever of ACP is as follows

$$EI\frac{\partial^4 w(x,t)}{\partial x^4} + \rho A\frac{\partial^2 w(x,t)}{\partial t^2} = 0 \quad -L_1 \le x \le 0 \ , \ 0 \le x \le L_2 \tag{1}$$

where A and I are the area and the area moment of inertia of the cross section, E is the modulus of elasticity and ρ is the volume density. The boundary conditions are derived as follows

$$w(-L_1,t) = \frac{\partial w(-L_1,t)}{\partial x} = 0 \tag{2}$$

$$EI\frac{\partial^2 w(L_2,t)}{\partial x^2} = EI\frac{\partial^3 w(L_2,t)}{\partial x^3} = 0 \tag{3}$$

the continuity conditions are written as follows

$$w(0^-,t) = w(0^+,t) \ , \ \frac{\partial w(0^-,t)}{\partial x} = \frac{\partial w(0^+,t)}{\partial x} \tag{4}$$

$$EI\frac{\partial^3 w(0^-,t)}{\partial x^3} - EI\frac{\partial^3 w(0^+,t)}{\partial x^3} = F_q cos\theta + F_p sin\theta + M_e\frac{\partial^2 w_G}{\partial t^2} \tag{5}$$

$$EI\frac{\partial^2 w(0^-,t)}{\partial x^2} - EI\frac{\partial^2 w(0^+,t)}{\partial x^2} = -EI\frac{\partial^3 w(0^+,t)}{\partial x^3}b + \left(F_q cos\theta + F_p sin\theta\right)\kappa_1 + \left(F_q sin\theta - F_p cos\theta\right)\kappa_2 + \frac{1}{2}M_e\frac{\partial^2 w_G}{\partial t^2}\kappa_3 - J_e\frac{\partial^3 w}{\partial x \partial t^2} \quad (6)$$

where

$$\begin{cases} \kappa_1 = Hcos\alpha + hsin\alpha \\ \kappa_2 = \frac{H}{2}sin\alpha - hcos\alpha \\ \kappa_3 = Hcos\alpha - d \\ w_G = w(0^-,t) - \frac{H}{2}\cos(\alpha)\frac{\partial w(0^-,t)}{\partial x} \end{cases} \quad (7)$$

also J_e in Eq. (6) is equal to $\frac{1}{3}M_e H^2$ which is the mass moment of inertia of the extension, and M_e is the mass of the extension [23].w_G is the extension center of gravity displacement along the *y* axis. F_p and F_q in Eq. (5) and Eq. (6) are interaction forces between the tip and the sample in the *p* and *q* directions, respectively and are defined as

$$\begin{cases} F_p = k_n\delta_p + C_n\frac{d\delta_p}{dt} \\ F_q = k_L\delta_q + C_L\frac{d\delta_q}{dt} \end{cases} \quad (8)$$

and δ_p and δ_q which are displacements of tip end normal and parallel to the sidewall surface will be as follows:

$$\begin{cases} \delta_p = w(0,t)\,sin\,\theta + Hsin(\alpha-\theta)\frac{\partial w(0,t)}{\partial x} - hcos(\alpha-\theta)\frac{\partial w(0,t)}{\partial x} \\ \delta_q = w(0,t)\,cos\,\theta + Hcos(\alpha-\theta)\frac{\partial w(0,t)}{\partial x} - hsin(\alpha-\theta)\frac{\partial w(0,t)}{\partial x} \end{cases} \quad (9)$$

Because the extension is not exactly located at the end of the cantilever, the cantilever is modelled as two beams. Thus, by assuming a solution of the form $y(x,t) = Y(x)e^{i\omega t}$ and $z(x,t) = Z(x)e^{i\omega t}$ for the left and right sides of the extension, respectively, and substituting the solution into Eq. 1, two ordinary differential equations for the mode functions are derived as follows

$$\frac{d^4Y(x)}{dx^4} - \beta^4 Y(x) = 0 \qquad -L_1 \le x \le 0 \quad (10)$$

$$\frac{d^4Z(x)}{dx^4} - \beta^4 Z(x) = 0 \qquad 0 \le x \le L_2$$

where $\beta^4 = \frac{\rho A}{EI}\omega^2$ is the flexural wave number and ω is the angular frequency. The following boundary and continuity conditions are thus obtained

$$Y(-L_1) = \frac{dY(-L_1)}{dx} = 0 \quad (11)$$

$$\frac{d^2Z(L_2)}{dx^2} = \frac{d^3Z(L_2)}{dx^3} = 0 \quad (12)$$

$$Y(0) = Z(0) \tag{13}$$

$$\frac{dY(0)}{dx} = \frac{Z(0)}{dx} \tag{14}$$

$$L^3 \frac{d^3Y(0)}{dx^3} + P_1 \frac{dY(0)}{dx} + P_2 Y(0) = L^3 \frac{d^3Z(0)}{dx^3} \tag{15}$$

$$L^3 \frac{d^2Y(0)}{dx^2} + q_1 \frac{dY(0)}{dx} + q_2 Y(0) = L^3 \frac{d^2Z(0)}{dx^2} - L^3 d \frac{d^3Z(0)}{dx^3} \tag{16}$$

where

$$\begin{cases} P_1 = -\frac{1}{2} M_f \gamma^4 H cos\alpha + r_2 \\ P_2 = M_f \gamma^4 - r_1 \\ q_1 = r_2 \kappa_1 + r_4 \kappa_2 - \frac{1}{4} M_f \gamma^4 \kappa_3 H cos\alpha - J_f H^2 \gamma^4 \\ q_2 = \frac{1}{2} M_f \gamma^4 \kappa_3 - r_1 \kappa_1 - r_3 \kappa_2 \end{cases} \tag{17}$$

$$\begin{cases} r_1 = \acute{\eta}_L cos^2\theta + \acute{\eta}_n sin^2\theta \\ r_2 = -\acute{\eta}_n u_2 sin\theta + \acute{\eta}_L u_1 cos\theta \\ r_3 = \frac{1}{2} sin2\theta (\acute{\eta}_L - \acute{\eta}_n) \\ r_4 = \acute{\eta}_L u_1 sin\theta + \acute{\eta}_n u_2 cos\theta \end{cases} \tag{18}$$

$$\begin{cases} u_1 = H cos(\alpha - \theta) + h sin(\alpha - \theta) \\ u_2 = H sin(\alpha - \theta) - h cos(\alpha - \theta) \end{cases} \tag{19}$$

In the above equations, $\gamma = \beta L$ is the normalized wave number. η_n and η_L are functions containing the normal and lateral contact stiffness and interaction damping, respectively:

$$\eta_n = k_n + i\omega C_n \quad , \quad \eta_L = k_L + i\omega C_L \tag{20}$$

also the dimensionless variables used in the Eq. (17)-(19) are defined as

$$\begin{aligned} &\acute{\eta}_L = \frac{\eta_L}{k_c} = \beta_L + i\zeta_L \quad , \quad \acute{\eta}_n = \frac{\eta_n}{k_c} = \beta_n + i\zeta_n \\ &k_c = \frac{EI}{L^3} \quad , \quad \beta_L = \frac{k_L}{k_c} \quad , \quad \beta_n = \frac{k_n}{k_c} \quad , \quad \zeta_L = \frac{\omega C_L}{k_C} \\ &\zeta_n = \frac{\omega C_n}{k_C} \quad , \quad M_f = \frac{M_e}{\rho AL} \quad , \quad J_f = \frac{J_e}{\rho AL H^2} \end{aligned} \tag{21}$$

A general solution of Eq. (10) can be expressed in the form

$$\begin{aligned} Y(x) &= C_1 sin\beta x + C_2 sinh\beta x + C_3 cos\beta x + C_4 cosh\beta x \\ Z(x) &= D_1 sin\beta x + D_2 sinh\beta x + D_3 cos\beta x + D_4 cosh\beta x \end{aligned} \tag{22}$$

substituting the boundary conditions of Eqs. (11) and (12) into Eq. (14), the general solution can be simplified

$$Y(x) = C_1[sin\beta(x+L_1) - sinh\beta(x+L_1)] + C_2[cos\beta(x+L_1) - cosh\beta(x+L_1)]$$
$$Z(x) = D_1[sin\beta(x-L_2) + sinh\beta(x-L_2)] + D_2[cos\beta(x-L_2) + cosh\beta(x-L_2)] \quad (23)$$

after lengthy manipulation, from continuity Eqs. (13-16)

$$\Delta_{11}D_1 + \Delta_{12}D_2 = 0$$
$$\Delta_{21}D_1 + \Delta_{22}D_2 = 0 \quad (24)$$

Where

$$\Delta_{11} = h_1F_1 + h_2G_1 + h_3 \qquad \Delta_{12} = h_1F_2 + h_2G_2 + h_4$$
$$\Delta_{21} = k_1F_1 + k_2G_1 + k_3 \qquad \Delta_{22} = k_1F_2 + k_2G_2 + k_4 \quad (25)$$

And

$$F_1 = -\left(cos\gamma - sin\frac{\gamma C_p}{1+C_p}sinh\frac{\gamma}{1+C_p} + cosh\gamma - cosh\frac{\gamma C_p}{1+C_p}cos\frac{\gamma}{1+C_p} + cos\frac{\gamma C_p}{1+C_p}cosh\frac{\gamma}{1+C_p} - sinh\gamma Cp1+Cpsin\gamma 1+Cp/21+cos\gamma Cp1+Cpcosh\gamma Cp1+Cp\right.$$

$$F_2 = -\left(sin\gamma - sin\frac{\gamma C_p}{1+C_p}cosh\frac{\gamma}{1+C_p} + sinh\gamma + cosh\frac{\gamma C_p}{1+C_p}sin\frac{\gamma}{1+C_p} + cos\frac{\gamma C_p}{1+C_p}sinh\frac{\gamma}{1+C_p} - sinh\gamma Cp1+Cpcos\gamma 1+Cp/21+cos\gamma Cp1+Cpcosh\gamma Cp1+Cp\right.$$

$$G_1 = \left(sin\gamma + cos\frac{\gamma}{1+C_p}sinh\frac{\gamma C_p}{1+C_p} - sinh\gamma - cosh\frac{\gamma}{1+C_p}sin\frac{\gamma C_p}{1+C_p} - cos\frac{\gamma C_p}{1+C_p}sinh\frac{\gamma}{1+C_p} + cosh\gamma Cp1+Cpsin\gamma 1+Cp/21+cos\gamma Cp1+Cpcosh\gamma Cp1+Cp\right.$$

$$G_2 = \left(cos\gamma - sin\frac{\gamma}{1+C_p}sinh\frac{\gamma C_p}{1+C_p} - cosh\gamma - sinh\frac{\gamma}{1+C_p}sin\frac{\gamma C_p}{1+C_p} - cos\frac{\gamma C_p}{1+C_p}cosh\frac{\gamma}{1+C_p} + cosh\gamma Cp1+Cpcos\gamma 1+Cp/21+cos\gamma Cp1+Cpcosh\gamma Cp1+Cp\right.$$

$$h_1 = -\gamma^3\left(cos\frac{\gamma}{1+C_p} + cosh\frac{\gamma}{1+C_p}\right) + \frac{P_1\gamma}{L}\left(cos\frac{\gamma}{1+C_p} - cosh\frac{\gamma}{1+C_p}\right) + P_2 \times \left(sin\frac{\gamma}{1+C_p} - sinh\frac{\gamma}{1+C_p}\right)$$

$$h_2 = \gamma^3\left(sin\frac{\gamma}{1+C_p} - sinh\frac{\gamma}{1+C_p}\right) - \frac{P_1\gamma}{L}\left(sin\frac{\gamma}{1+C_p} + sinh\frac{\gamma}{1+C_p}\right) + P_2 \times \left(cos\frac{\gamma}{1+C_p} - cosh\frac{\gamma}{1+C_p}\right)$$

$$h_3 = \gamma^3\left(cos\frac{\gamma C_p}{1+C_p} - cosh\frac{\gamma C_p}{1+C_p}\right)$$

$$h_4 = \gamma^3\left(sin\frac{\gamma C_p}{1+C_p} + sinh\frac{\gamma C_p}{1+C_p}\right)$$

$$k_1 = -\frac{q_1\gamma^2}{L^2}\left(sin\frac{\gamma}{1+C_p} + sinh\frac{\gamma}{1+C_p}\right) + \frac{q_2\gamma}{L}\left(cos\frac{\gamma}{1+C_p} - cosh\frac{\gamma}{1+C_p}\right)$$

$$k_2 = -\frac{q_1\gamma^2}{L^2}\left(cos\frac{\gamma}{1+C_p} + cosh\frac{\gamma}{1+C_p}\right) - \frac{q_2\gamma}{L}\left(sin\frac{\gamma}{1+C_p} + sinh\frac{\gamma}{1+C_p}\right)$$

$$k_3 = \gamma^3 d\left(-cos\frac{\gamma C_p}{1+C_p} + cosh\frac{\gamma C_p}{1+C_p}\right) + \gamma^2 L\left(-sin\frac{\gamma C_p}{1+C_p} + sinh\frac{\gamma C_p}{1+C_p}\right)$$

$$k_4 = -\gamma^3 d\left(sin\frac{\gamma C_p}{1+C_p} + sinh\frac{\gamma C_p}{1+C_p}\right) + \gamma^2 L\left(cos\frac{\gamma C_p}{1+C_p} - cosh\frac{\gamma C_p}{1+C_p}\right) \quad (26)$$

in the Eq. (26), $C_p = \frac{L_2}{L_1}$ is the connection position of the extension.
Regarding the above equations, the characteristic equation of the system is given by

$$C(\gamma, \beta_l) = \Delta_{11}\Delta_{22} - \Delta_{12}\Delta_{21} \quad (27)$$

Therefore, the relation between frequency and wave number is given

$$f = \frac{\gamma^2}{2\pi L^2}\sqrt{\frac{EI}{\rho A}} \quad (28)$$

and finally, a dimensionless form of the flexural sensitivity is given by [24]

$$S_n = \frac{df/d\beta_L}{(1/2\pi L^2)\sqrt{EI/\rho A}} \quad (29)$$

For convenience, relative shifts of the frequency and sensitivity are defined and used in the analysis as follows

$$E_f = \frac{(f_2 - f_1)}{f_1} \times 100\% \quad (30)$$

$$E_s = \frac{(S_{n2} - S_{n1})}{S_{n1}} \times 100\% \quad (31)$$

RESULTS AND DISCUSSION

In this study, the flexural sensitivity and resonant frequency of the vibration modes of an inclined AFM cantilever with a sidewall probe have been analyzed and the closed-form expressions have also been obtained, taking into account the effects of the various parameter, such as the slope of the cantilever, the angle between the extension and cantilever, the connection position of the extension and the damping. A good analysis must consider all of the parameters simultaneously. The flexural sensitivity is defined as the change in the flexural vibration frequency of a mode with respect to the change in contact stiffness [19]. In order to analyze the effect of these parameters on the flexural sensitivity and resonant frequency, we considered the geometric and material parameters as $E = 170GPa,\ \rho = 2300\frac{Kg}{m^3}, a = 50\,\mu m,\ b = 2\,\mu m,\ L = 300\,\mu m,\ h = 10\mu m,\ H = 150\mu m$ $and\ C_L = 10^{-5}$. The normal contact stiffness and damping was assumed as$K_n = 0.9K_L, C_n = 0.8C_L$.

The resonant frequency of the first vibration mode for the various connection position of the extension is shown in Figure 2. As it can be seen, the resonant frequency is equal to the free resonance frequency for very low values of β_L. As β_L increases, the frequency rapidly increases until it eventually reaches a constant value at a very high value of contact stiffness. It can also be seen that the effect of connection position is not significant

for the low values of contact stiffness. By gradually increasing the contact stiffness of the system, the effect of increasing the connection position of the extension is that the resonant frequency also rises.

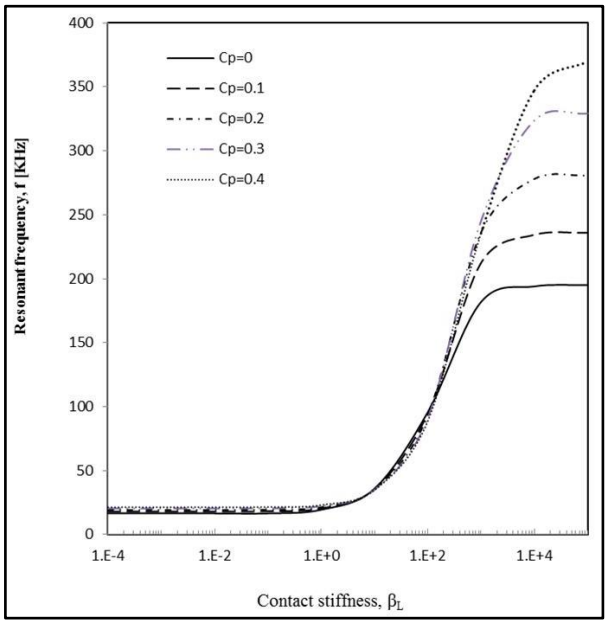

Fig. 2. The resonant frequency of the first mode as a function of contact stiffness at various values of connection position

Figure 3 illustrates the change in the first normalized flexural sensitivity due to the change in β_L and the connection position of the extension. The figure reveals that the greatest flexural modal sensitivity occurs at a small contact stiffness of the system, in which the connection position is also small.

The normalized flexural sensitivities, S_n of the first four vibration modes for an AFM cantilever are depicted in Figure 4. With a short glance, it can be found that the first mode is most sensitive to changes in surface stiffness. It can also be found that the maximum values for the sensitivities of the first four modes are 0.28398, 0.003527, 0.005119, and 0.001247. When β_L exceeds 120, the sensitivity of the first mode is smaller than that of the second mode and the second mode experiences the largest shifts in the frequency rather than other modes. By increasing the contact stiffness, a similar phenomenon was found at other higher mode and the sensitivity of higher mode will be more sensitive than lower one.

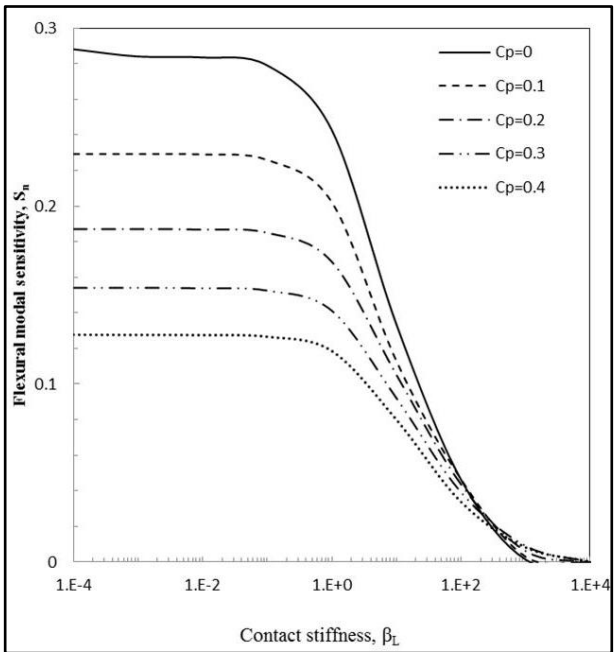

Fig. 3. The normalized flexural modal sensitivity of the first mode as a function of contact stiffness for an ACP at various values of connection position

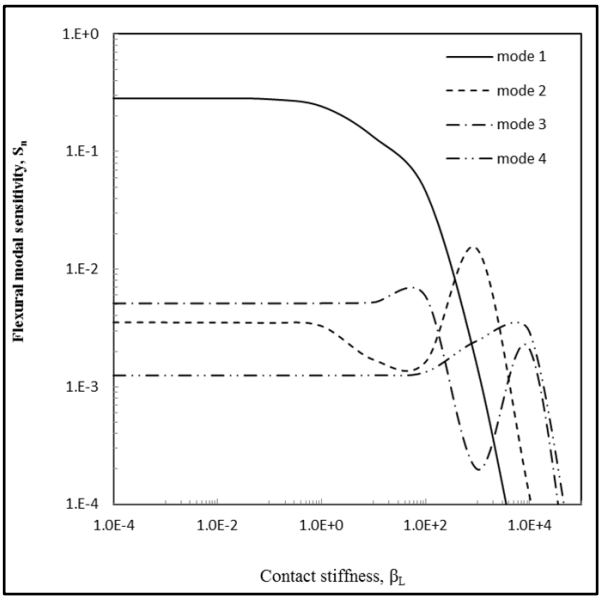

Fig. 4. The normalized flexural modal sensitivity as a function of contact stiffness for the first four modes

Figure 5 shows the relative shift of the resonant frequency for the first three modes of damped and undamped systems. At low values of contact stiffness, the effect of damping on the resonant frequency is considerable, especially for

the first mode. It can be seen from this figure that the maximum values of the relative shift of the first three resonant frequencies are 137, 182, and 211 percent, respectively. However, the effect of damping on the first resonant frequency rapidly decreases with an increase in the contact stiffness. When, the value of β_L reaches approximately 1, the sensitivity of mode 2 is greater than mode 1. A similar phenomenon is found at other higher mode. For higher values of β_L, the effect of damping on the resonant frequency of higher mode is more than that of the lower one.

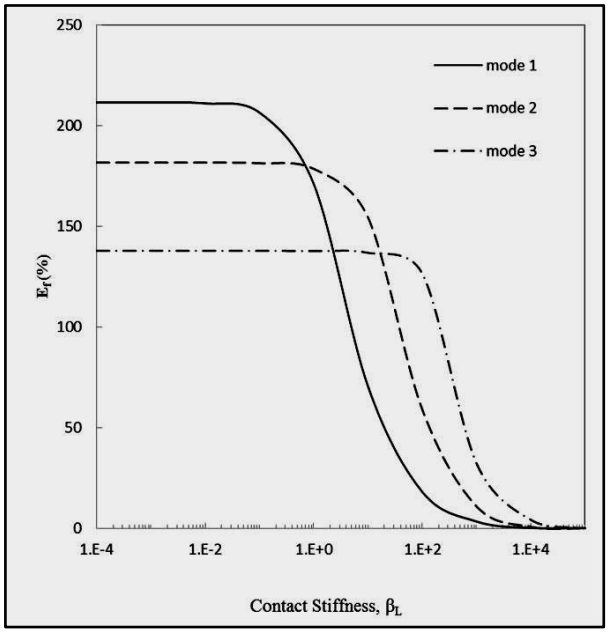

Fig. 5. A relative shift of resonant frequency for the first three modes as a function of contact stiffness: (1) undamped; (2) damped.

The effect of damping on the first flexural modal sensitivity is illustrated in Figure 6. It can be inferred that the interacting damping decreases the flexural sensitivity dramatically at low value of contact stiffness.

The effects of cantilever and extension angles (α and θ) on the resonant frequency and the flexural modal sensitivity at various length ratios of the cantilever and extension, H/L are investigated in Figures 7 and 8. Two different cases are considered in these figures. In the first case, the relative shifts of the frequency, E_f and the sensitivity, E_s are analyzed for 15° shift of the extension angle, α from 90° to 75° when the cantilever is horizontal. In the second case, the relative shifts of the frequency, E_f and the sensitivity, E_s are analyzed for 15° shift of the cantilever angle, θ, from 0° to15° when the extension angle is vertical. In both cases, three values for the length ratios of the cantilever and the extension H/L are considered as 0.2, 0.5 and 0.8. The figures reveal that the relative shifts of the frequency, E_f and the sensitivity, E_s are not considerable when the contact stiffness, β_L exceeds 100. Also, increasing the $/L$, increases the relative shifts of either the frequency or the sensitivity. It can be found from Figure 7 that the change in the extension angle, α is more effective on the resonant frequency in comparison to the change in the cantilever angle, θ particularly at higher values of H/L. The situation is different in Fig. 8. In this figure, the effect of change in the cantilever angle on the relative shift of sensitivity is more than the change in the extension angle when the H/L is low. By increasing the H/L incrementally, the shift in the extension angle is more effective on the relative shift of sensitivity.

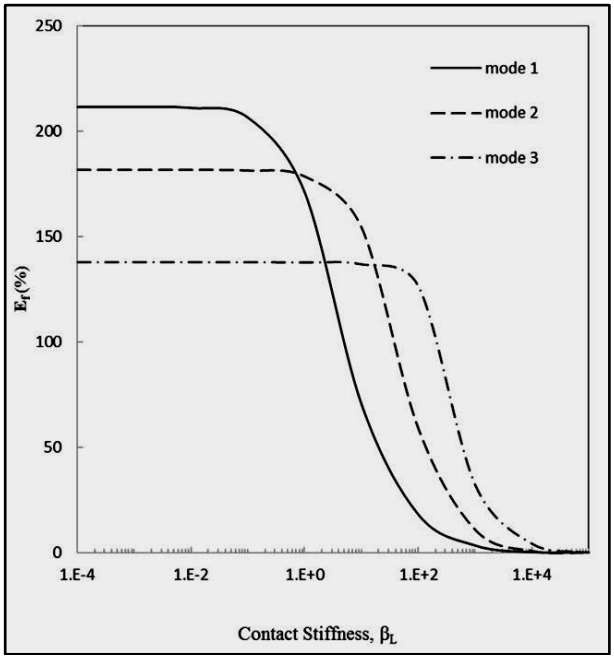

Fig. 6. The effect of damping on the normalized flexural modal sensitivity as a function of contact stiffness for an ACP.

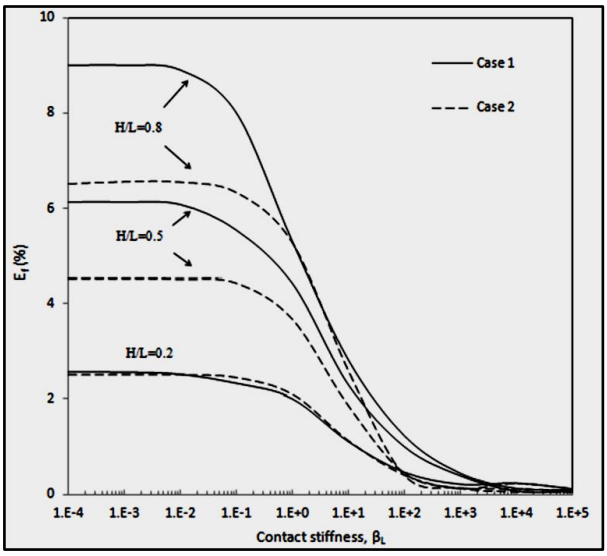

Fig. 7. A relative shift of the resonant frequency of mode1 as a function of contact stiffness at various length ratios of the cantilever and the extension, $\boldsymbol{H/L}$ and for two cases; case 1: a $\mathbf{15}^{\circ}$ shift of extension angle, $\boldsymbol{\alpha}$, from $\mathbf{90}^{\circ}$ to$\mathbf{75}^{\circ}$; case 2: a $\mathbf{15}^{\circ}$ shift of cantilever angle, $\boldsymbol{\theta}$, from $\mathbf{0}^{\circ}$ to$\mathbf{15}^{\circ}$.

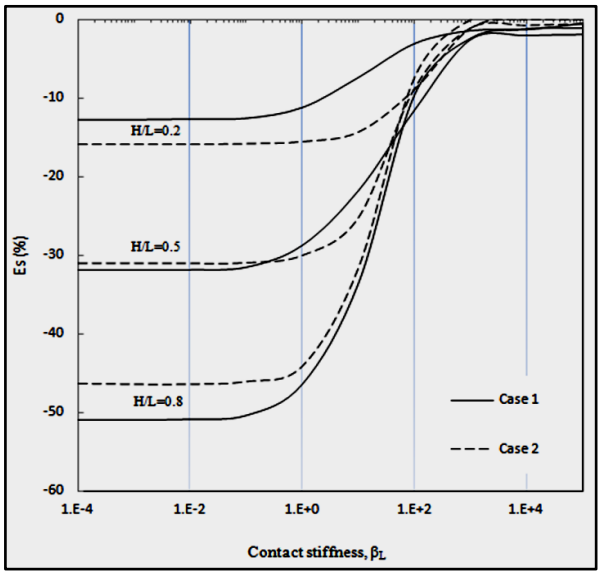

Fig. 8. A relative shift of the normalized flexural modal sensitivity of mode1 as a function of contact stiffness at various length ratios of the cantilever and the extension, $\boldsymbol{H/L}$ and for two cases; case 1: a $\mathbf{15}^{\circ}$ shift of extension angle, $\boldsymbol{\alpha}$, from $\mathbf{90}^{\circ}$ to$\mathbf{75}^{\circ}$; case 2: a $\mathbf{15}^{\circ}$ shift of cantilever angle, $\boldsymbol{\theta}$, from $\mathbf{0}^{\circ}$ to$\mathbf{15}^{\circ}$.

CONCLUSIONS

In this paper, the effects of the interaction stiffness and damping, and the geometrical parameters of the cantilever and extension on the resonant frequencies and flexural sensitivities of an atomic force microscope cantilever with a sidewall probe have been analyzed. According to the analysis, the first mode is the most sensitive mode when the contact stiffness is low. However, the high-order flexural vibration modes are more sensitive than the first mode when the contact stiffness is greater. The results indicated that at high values of contact stiffness, the resonant frequency increases as the connection position increases. On the other hand, the connection position is effective on the flexural modal sensitivity at the low values of contact stiffness. At this situation, the flexural sensitivity is higher when the extension is close to the free end of the cantilever. The results also showed that the effects of damping on the flexural sensitivity are considerable and cannot be neglected when the contact stiffness is lower. Finally, it was observed that at low values of contact stiffness, the effects of changes in the cantilever angle, θ and the extension angle, α are significant especially for the flexural modal sensitivity and are the functions of the H/L.

REFERENCES

[1] Mazeran P. E., Loubet J. L., (1999), Normal and lateral modulation with a scanning force microscope, an analysis: implication in quantitative elastic and friction imaging. *Tribology Lett.* 7: 199-212.

[2] Garcia R., (2010), *Amplitude Modulation Atomic Force Microscopy*, First ed., Germany: Wiley-VCH.

[3] Albrecht T. R., Akamine S., Carver T. E., Quate C. F., (1990), Microfabrication of cantilever for the atomic force microscope. *J. Vac. Sci. Technol. A-Vac. Surf. Films.* 8: 3386–3396.

[4] Chang C. T., Lin K., Ju M. S., (2013), Combine atomic force and fluorescence microscopies to measure subcellular mechanical properties of lives cells. *J. Mech. Medic. Biol.* 13: 1350057-9

[5] Wu T.-S., Chang W.-J., Hsu J.-C., (2004), Effect of tip length and normal and lateral contact stiffness on the flexural vibration responses of atomic force microscope cantilevers. *Microelec. Eng.* 71: 15-20.

[6] Kahrobaiyan M. H., Asghari M., Rahaeifard M., Ahmadian M. T., (2010), Investigation of the size-dependent dynamic characteristics of atomic force microscope microcantilevers based on the modified couple stress theory. *Int. J. Eng. Sci*. 48: 1985-1994.

[7] Korayem M. H., Ebrahimi N., Sotoudegan M. S., (2011), Frequency response of atomic force microscopy microcantilevers oscillating in a viscous liquid: A comparison of various methods. *Scientia Iranica.* 18: 1116-1125.

[8] Abbasi M., Karami Mohammadi A., (2009), Effect of contact position and tip properties on the flexural vibration responses of atomic force microscope cantilevers. *IREME.* 3: 196-202.

[9] Georgakaki D., Mitridis S., Sapalidis A. A., Mathioulakis E., Polatoglou H. M., (2013), Calibration of tapping AFM cantilevers and uncertainty estimation: Comparison between different methods. *Meas. Sci. Tech.* 46: 4274-4281.

[10] Chang W., (2002), Sensitivity of Vibration Modes of Atomic Force Microscope Cantilevers in Continuous Surface Contact. *Nanotechnol.* 13: 510-514.

[11] Abbasi M., Karami Mohammadi A., (2010), A new model for investigating the flexural vibration of an atomic force microscope cantilever. *Ultramicroscopy.* 110: 1374-1379.

[12] Chang W.-J., Fang T.-H., Chou H.-M., (2003), Effect of interactive damping on sensitivity of vibration modes of rectangular AFM cantilevers. *Phys. Lett. A.* 312: 158-165.

[13] Mahdavi M. H., Farshidianfar A., Tahani M., Mahdavi S., Dalir H., (2008), A more comprehensive modeling of atomic force microscope cantilever. *Ultramicroscopy.* 109: 54-60.

[14] Lee H. W., Chang W. J., (2008), Coupled lateral bending–torsional vibration sensitivity of atomic force microscope cantilever. *Ultramicroscopy.* 108: 707–711.

[15] Lin S. M., (2010), Effective dampings and frequency shifts of several modes of an inclined cantilever vibrating in viscous fluid. *Precis. Eng.* 34: 320-326.

[16] Korayem M. H., Kavousi A., Ebrahimi N., (2011), Dynamic analysis of tapping-mode AFM considering capillary force interactions. *Sci. Iranica.* 18: 121-129.

[17] Abbasi M., Afkhami S. E., (2015), Resonant Frequency and Sensitivity of a Caliper Formed With Assembled Cantilever Probes Based on the Modified Strain Gradient Theory. *Micros. Microanal.* 20:1672–1681.

[18] Dai G., Wolff H., Pohlenz F., Danzebrink H. U., Wilkening G., (2006), Atomic force probe for sidewall scanning of nano- and microstructures. *Appl. Phys. Lett.* 88: 171908-11.

[19] Chang W. J., Lee H. L., Chen T. Y., (2008), Study of the sensitivity of the first four flexural modes of an AFM cantilever with a sidewall probe. *Ultramicroscopy.* 108: 619-24.

[20] Abbasi M., Karami Mohammadi A., (2014), A Detailed Analysis of the Resonant Frequency and Sensitivity of Flexural Modes of Atomic Force Microscope Cantilevers with a Sidewall Probe Based on a Nonlocal Elasticity Theory. *Strojniški vestnik – J. Mech. Eng.* 60: 179-186.

[21] Kahrobaiyan M. H., Ahmadian M. T., Haghighi P., Haghighi A., (2010), Sensitivity and resonant frequency of an

AFM with sidewall and top-surface probes for both flexural and torsional modes. *Int. J. Mech. Sci.* 52: 1357-1365.

[22] Dai G., Wolff H., Weimann T., Xu M., Pohlenz F., Danzebrink H. U., (2007), Nanoscale surface measurements at sidewalls of nano- and micro-structures. *Meas. Sci. Technol.* 18: 334-341.

[23] Beer F. P., Johnston E. R. (1981). *Mech. Mater*. New York: McGraw-Hill.

[24] Turner J. A., Wiehn J. S., (2001), Sensitivity of Flexural and Torsional Vibration Modes of Atomic Force Microscope Cantilevers to Surface Stiffness Variation. *Nanotechnol.* 12: 322-330.

Cite this article as: M. Abbasi: Study of the flexural sensitivity and resonant frequency of an inclined AFM cantilever with sidewall probe.
Int. J. Nano Dimens. 6 (4): 351-362, Autumn 2015.